國立臺灣海洋大學食品科學系碩士班

專題討論書面報告

探討噴霧感染流感病毒對動物之影響

授課老師：柯源悌 老師　張君如 老師

指導老師：吳彰哲 老師

學　　號：10732060

學　　生：羅凱隆 (5136)

報告日期：108 年 4 月 10 日

內容 40%	時間掌控 10%	表達能力 30%	投影片 10%	書面資料 10%

探討噴霧感染流感病毒對動物之影響

羅凱隆 (5136)

2019/4/10

大綱

摘要

A 型流感病毒（Influenza A virus, IAV）屬於正黏液病毒科（Orthomyxoviridae），是一種感染人類和動物並可能導致全球大流行的主要病原體，感染會造成傳染性呼吸道疾病且具有高發病率及高死亡率。流感的傳染途徑，主要是透過感染者咳嗽或打噴嚏所產生的飛沫將病毒傳播給其他人，尤其在密閉空間，由於空氣不流通，更容易造成病毒傳播。高致病性禽流感（H5N1）病毒的感染人類通常會致命，但疾病的機制仍然不明確。常規氣管內接種流感病毒在非人靈長類動物中可能導致上呼吸道內病毒的被清除，並無法產生嚴重疾病。霧化的流感病毒會導致肺泡巨噬細胞被破壞，並引起間質巨噬細胞和中性粒細胞的流入肺泡，推斷病毒的小顆粒 Aerosol 會穿透下呼吸道和覆蓋肺泡。在獼猴吸入霧化的流感病毒會導致暴發性肺炎發展為急性呼吸窘迫綜合症，與人類疾病相符，可於更廣泛的研究。用甲型流感（H1N1）病毒比較兩種感染途徑，氣管噴霧途徑的絨猴中，整個肺部和氣管中發現了炎症。常規途徑的絨猴中，肺部只有局部發炎，結果表明，氣管噴霧途徑比常規途徑更合適接種流感病毒。為評估不同流感病毒的感染途徑對雞的影響，用四種低致病性 H6N1 、 H10N7 、 H10N8 和 H13N6 病毒分別通過噴霧、常規途徑感染。流感病毒的感染方式都以常規的滴鼻腔、眼睛、口服等為主，但常規方法卻只能造成肺部局部的感染，跟自然狀態下差別極大，噴霧方式感染能平均的感染肺部，進而誘導出更多的併發症，可用於更廣泛的研究。

一、前言

A 型流感病毒（Influenza A virus, IAV）屬於正黏液病毒科(Orthomyxoviridae)，其基因體含 8 段(A、B 型)或 7 段(C 型)負向單股 RNA，可依 NP 及 M 蛋白可分為 A 型、 B 型及 C 型。流感病毒是一種感染人類與動物的病原體。在 2009 年墨西哥發現的新型流感(H1N1)迅速地傳播到世界各地，具有高發病率及高死亡率，感染會造成傳染性呼吸道疾病。流感的症狀包括發燒、頭痛、流鼻水、喉嚨痛、咳嗽、肌肉酸痛及疲倦等。高危險群的病患，可能引發嚴重併發症，甚至導致死亡。有些人感染流感病毒後可能出現流感併發重症，如肺部、神經系統、心肌炎/心包膜炎或侵襲性細菌感染等嚴重併發症，而需住院治療，甚至導致死亡。根據世界衛生組織 (World Health Organization，WHO) 統計，每年併發重症人數約 300~500 萬，每年死亡人數約 25~50 萬人，多數死亡者為 65 歲以上老年人。流感的傳染途徑主要是透過感染者咳嗽或打噴嚏所產生的飛沫將病毒傳播給其他人，尤其在密閉空間，由於空氣不流通，更容易造成病毒傳播。另外，因為流感病毒可短暫存活於物體表面，所以也可經由接觸傳染，如手接觸到污染物表面上的口沫或鼻涕等黏液，再碰觸自己的口、鼻或眼睛而感染。

動物模型對於人類傳染病的研究相當重要，在流感病毒研究中，常用的感染方式為滴鼻腔、眼睛、口服等，但感染此當下，會因為打噴嚏、鼻涕、咳嗽將病毒排出，導致感染的病毒量有誤差及分布不均。噴霧感染，是一種較新的感染途徑，但仍然有許多問題與技術須要克服。

目前，噴霧感染已有眾多研究證實效果比常規感染好，為了更瞭解噴霧感染使用的動物模型之方法，本專討報告將探討噴霧感染流感病毒對於動物產生的各種影響，期待發現噴霧感染的最大效益。

二、獼猴以噴霧感染 H5N1 流感使肺泡中廣泛複製的病毒引起急性呼吸窘迫綜合症

本篇探討以噴霧方式感染高致病性的流感病毒 H5N1 是否能引起獼猴的急性呼吸窘迫綜合症(Wonderlich et al., 2017)。

使用健康成年雌性食蟹獼猴（ *Macaca fascicularis* ），手術植入 TA10TA-D70 遙測裝置以監測溫度和活動。用氯胺酮將獼猴麻醉，將獼猴頭部插入暴露室中，用 Aeroneb Solo 霧化器（Aerogen，Deerfield，IL）產生病毒氣霧劑，暴露持續時間為 15 至 34 分鐘。霧化器產生的平均粒徑為 4 μm，受感染的猴子有 3 隻因發病而死亡，4

隻在 2~6 天內犧牲，並收集鼻沖洗液、支氣管衝提液。病毒滴度在鼻沖洗液中的量非常低，而肺中的病毒量最高，顯示吸入的病毒雖是由鼻咽部感染，但病毒的複製主要不是在上呼吸道中 (Table 1)。體溫的變化量 (Fig. 1A)，感染後立即對呼吸功能產生影響，呼吸速率增加，潮氣量和呼氣時間減少 1-2 天 (Fig. 1B)。用氟代脫氧葡萄糖 (FDG) 為放射性顯影劑並使用正電子電腦斷層掃描 (PET) 顯像，及使用電腦斷層掃描 (CT) 顯示肺部結構，第 2 天顯示所有動物肺中發生嚴重的瀰漫性炎症， FDG 攝取和肺容量顯著增加(Fig. 1C，1D)。犧牲後觀察其肺部，可以看到肺泡內有炎性滲出液，相對於未感染對照，肺部體重增加 3 至 4 倍 (Fig. 2A-C)。測量肺中的細胞量，在感染和未感染的獼猴之間沒有差異 (Fig. 2D)。以半定量 RT-PCR 檢測在左右肺的病毒量沒有顯著差異，其他組織中也偵測出有病毒的存在，最顯著的是在肺門淋巴結 (Fig. 2E)。原位雜合技術證實，在大多數肺泡內的細胞中有大量的複制。在肺泡細胞、肺門淋巴結及十二指腸中都有檢測到病毒 RNA 存在，證實全身性感染 (Fig. 2F)。犧牲後取支氣管沖提液和血液使用流式細胞儀分析，血液分析後的結果 (Fig. 3A)，量化呈現在感染後第一和第二天血液中的白血球和 T 細胞顯著減少，而單核球的數量則顯著上升(Fig. 3B)。分析支氣管沖提液，將沖提液中細胞定量 (Fig. 3C)，沖提液中細胞量不因感染而改變。細胞組成顯著改變 (Fig. 3D)，以量化呈現 (Fig. 3E)，支氣管沖提液分別測定肺泡巨噬細胞、肺間質巨噬細胞及顆粒球，感染前有約 50%為肺泡巨噬細胞，感染後肺巨噬細胞下降，間質巨噬細胞在感染前後都沒有顯著表現，檢測血液和支氣管沖提液中的促發炎因子和趨化因子 (Fig. 3F-G)，血液中的促發炎因子短暫的增加，在支氣管沖提液中所有的促炎因子和趨化因子都顯著上升。在感染的前期 IFN -α 的表現量提高了約 3000 倍 (Fig. 3H)，但 H5N1 病毒仍能拮抗 IFN 的基因表達，導致肺泡破壞。犧牲後取其肺組織以流式細胞儀進行分析，分別測定懸浮液中的肺泡上皮細胞、肺泡巨噬細胞、間質巨噬細胞、嗜中性球、漿細胞樣樹突細胞及樹突狀細胞；在感染的獼猴中，肺泡上皮細胞表現量降低，而肺泡巨噬細胞的表現量也下降與支氣管沖提液的結果相同，間質巨噬細胞與嗜中性球則增加，樹突狀細胞表現量沒有差異，而漿細胞樣樹突細胞表現則下降(Fig. 4A-B)，檢測肺泡及間質中的 Ki-67 蛋白 (Fig. 4C)，量化呈現 (Fig. 4D)，結果顯示感染後在間質中觀察到 Ki-67 蛋白顯著升高；肺部切片的免疫螢光染色 (Fig. 4E)，在感染後間質巨噬細胞與嗜中性球表現增加，結果與流式細胞儀相同；肺泡上皮細胞和嗜中性球在感染後會產生

IFN-α和 MCP-1 的表達 (Fig. 4F)，但在間質中則沒有表現。觀察在組織中 H5N1 感染細胞的狀況 (Fig. 5A)，可看到在 I 型及 II 型肺泡中有大量的病毒存在，在肺泡中有少量的肺泡巨噬細胞，有檢測到病毒存在，在流式細胞儀中肺上皮細胞有約 20%被病毒感染，肺泡巨噬細胞有>30%，間質巨噬細胞則只有 5%被病毒感染 (Fig. 5B-C)，在圖中顯示感染後的肺上皮細胞 caspase-3 活性較高(Fig. 5D)，表示感染會造成肺上皮細胞的凋亡，在感染第二天觀察支氣管衝提液中的白蛋白濃度增加 20 倍 (Fig. 5E)，在感染第 4 到 6 天白蛋白濃度持續上升，但在血漿中的白蛋白濃度卻不因感染而有改變。

作者認為在非人類靈長類動物中，常規方法感染流感病毒 H5N1 時，很少會引發急性呼吸窘迫綜合症。常規使用滴鼻腔、眼睛等方法不太可能將足以引起其他病症的病毒量送入肺泡當中，病毒可能會被上呼吸道的黏液、纖毛清除。本實驗證實，食蟹獼猴在吸入霧化為直徑 5 μm 的病毒小顆粒時，能夠有效地引起與人類相符的急性呼吸窘迫症。

三、以絨猴做為流感動物模型：通過常規或噴霧模式感染流感（H1N1）pdm09 和高致病性（H5N1）病毒

本篇目的為檢測常規途徑與氣管噴霧途徑的差異及絨猴對 H5N1 的敏感度 (Iwatsuki-Horimoto et al., 2018)。

將三至八歲的雌性普通絨猴用異氟烷麻醉，H1N1 以常規途徑及氣管噴霧途徑感染；H5N1 則以氣管噴霧途徑感染。檢測呼吸道中的唾液酸寡糖分佈。在鼻甲，咽，氣管，支氣管，細支氣管和肺泡中，沒有組織與 SNA I 反應，但有檢測到 MAA II 的結合 (Fig. 6)。感染 H1N1 絨猴鼻液中的病毒滴度 (Table 2)，通過氣管噴霧途徑感染的動物有一隻完全沒有排出病毒，剩下的動物皆從鼻腔中排出病毒。H1N1 感染絨猴的電腦斷層掃描 (Fig. 7)及通過氣管噴霧途徑感染發炎分布均勻、常規途徑感染只有局部發炎。受感染 H5N1 的絨猴的體重和體溫的變化 (Fig. 8)中，在第一天顯示出突然的體重減輕及體溫下降，但之後都恢復正常。受感染絨猴器官中的病毒滴度(Table 3)，第三天時，在所有呼吸器官和其他內臟器官中均檢測到高滴度的 H5N1 ，第六天時，病毒滴度在許多器官中下降；然而，其中一隻動物的病毒是從大腦中回收的。通過免疫組織化學檢測的抗原陽性細胞的分佈 (Table 4)，顯示出與病毒滴度幾乎相同的結果，在鼻甲和氣管中檢測到病毒抗原，心臟和肝臟檢測到抗原陽性細胞。H5N1 感

染絨猴的病理學檢查 (Fig. 9)，所有肺組織切片均顯示炎症，心臟和肝臟顯示局部炎症以及病毒抗原陽性細胞；在大腦中，顯示輕度炎症。絨猴腦的病理檢查 (Fig. 10)，免疫組織染色顯示病毒抗原呈陽性的神經細胞，特別是 CJ14 中室管膜細胞。H5N1 不僅在呼吸器官中感染和複製，而且還在心臟，肝臟和腦中感染和複製。

作者認為 H5N1 對於絨猴的感染不局限於肺，病毒還會在腦、心臟等進行複製。通過常規途徑感染流感病毒，會導致強烈的局部感染。反之，通過噴霧途徑感染病毒，在肺部中複製會比較平均。

四、Aerosol 增強禽類中低致病性流感病毒的感染

本篇探討在低致病性流感病毒使用噴霧感染是否能增強其感染效果(Jegede *et al.*, 2018)。

通過 Aerosol、鼻內或口服感染途徑研究各種器官組織中的病毒複製和細胞因子基因表達。共進行四次獨立實驗，每種病毒一次。用 H6N1、H10N7、H10N8 和 H13N6 病毒；鼻內或口服感染， H6N1 和 H10N7 病毒滴度為 1.58×10^{7} EID_{50} / mL，而 H10N8 和 H13N6 病毒 4.28×10^{6} 和 2.81×10^{6} EID_{50} / mL；Aerosol 接種，使用噴霧器和空氣壓縮機霧化病毒原液，將雞暴露於室中，噴入霧化病毒 15 分鐘。監測病毒脫落，第 1、3、7 天，從所有雞的口咽、泄殖腔中收集拭子。將拭子用逆轉錄聚合酶鏈反應測定病毒滴度。犧牲後，從氣管和肺組織樣品中提取的 RNA 用於合成 cDNA。基因作為參照評估干擾素 γ，介白素 1β 和介白素 6 基因的表達。

通過 Aerosol、鼻內或口服途徑感染 H6N1、H10N7 和 H10N8 病毒的雞的口咽腔中病毒複製 (Fig. 11)。Aerosol 或鼻內感染的雞中的病毒滴度顯著高於口服感染的雞 (Fig. 11A)，與口服感染相比，Aerosol 或鼻內接種 H6N1，H10N7 和 H10N8 病毒更有效地引起雞的口咽感染。通過 Aerosol、鼻內或口服感染 H6N1、H10N7 和 H10N8 病毒雞的氣管和肺組織中病毒複製路線 (Fig. 12)。第一和第三天，在 Aerosol 感染的雞氣管和肺組織中，H6N1 和 H10N8 病毒滴度顯著高於鼻內或口服感染的雞 (Fig. 12A-B)，相比之下，Aerosol 感染的雞肺中 H10N7 病毒複製僅在感染後第一天有顯增加 (Fig. 12C-D)。與鼻內或口服感染相比，Aerosol 感染更有效地將 H6N1，H10N7 和 H10N8 病毒遞送至雞的氣管和肺。通過 Aerosol、鼻內或口服途徑在感染 H6N1、H10N7 和 H10N8 病毒的雞盲腸中病毒的複製 (Fig. 13)。H6N1，H10N7 和 H10N8 病毒的複製在雞盲腸和泄殖腔中受到限制。感染後第三天口服感染 H10N8 病毒的雞盲腸

中沒有檢測到任何病毒 (Fig. 13E)。與口服接種相比，接受 Aerosol 或鼻內感染的雞 H10N8 滴度顯著更高。通過 Aerosol、鼻內或口腔途徑感染雞氣管和肺中的細胞因子 mRNA 對 H6N1 的反應 (Fig. 14)。感染 H6N1 或 H10N8 病毒的雞氣管和肺組織中評估細胞因子基因 IFN-γ，IL-6 和 IL-1β 的表達。這些器官組織中病毒複製中觀察到的差異有限，在感染 H10N7 或 H13N6 病毒的雞中不進行這種評估。通過 Aerosol、鼻內或口腔途徑感染雞氣管和肺至 H10N8 的細胞因子 mRNA 反應 (Fig. 15)。在整個 7 天的實驗中，在通過鼻內或口服途徑接種病毒的任何雞中未觀察到臨床症狀。然而，暴露於霧化的 H10N8 病毒的六隻雞中有兩隻死於第六天，並且暴露於霧化的 H6N1 病毒的六隻雞中有一隻死於第五天。

作者認為霧化的病毒會沿著氣流行進到下呼吸道，在肺中建立感染，通過雞的循環系統傳播到其他器官。霧化病毒比鼻內感染途徑與口服途徑有更高的病毒複製。可能是鼻內感染途徑的大尺寸病毒液滴限制了上呼吸道感染並產生輕度呼吸道疾病。口服感染後的病毒通過食道進入消化系統的其他器官。胃腸道中的酸性條件和消化酶可能在病毒附著和進入靶宿主細胞之前使病毒失活。因此，與鼻內或 Aerosol 途徑相比，通過口服感染途徑需要更高的病毒劑量。

五、結論

流感病毒的感染方式都是以常規的滴鼻腔、眼睛、口服等方式感染，但常規方法卻只能造成肺部局部的感染，跟自然狀態下差別極大；鼻腔攻毒會因感染劑量、體積、病毒株種類、動物年齡和病毒顆粒大小而有顯著差異。口服感染途徑效果最差，需要大量的病毒才有可能感染，會無法計算給予的病毒量，進而失敗。

而噴霧方式感染能平均的感染肺部，進而誘導出更多的併發症，比起常規途徑，可用於更廣泛的研究。

六、參考文獻

Bowes, V. A., Ritchie, S. J., Byrne, S., Sojonky, K., Bidulka, J. J., & Robinson,J. H. (2004). Virus characterization, clinical presentation, and pathology associated with H7N3 Avian Influenza in British Columbia broiler breeder chickens in 2004. *Avian Diseases*, 48(4), 928–934.

Chen, H., Li, Y., Li, Z., Shi, J., Shinya, K., Deng, G. (2006). Properties and dissemination of H5N1 viruses isolated during an influenza outbreak in migratory waterfowl in western China. *Journal of virology*, 80, 5976–5983.

Fan, S.,Gao, Y., Shinya, K., Li, C. K., Li, Y., Shi, J. (2009). Immunogenicity and protective efficacy of a live attenuated H5N1 vaccine in nonhuman primates. *PLoS Pathog.* 5:e1000409.

Guan, J., Fu, Q., & Sharif, S. (2015). Replication of an H9N2 avian influenza virus and cytokine gene expression in chickens exposed by aerosol or intranasal routes. *Avian Diseases*, 59(2), 263–268.

Itoh, Y., Shinya, K., Kiso, M., Watanabe, T., Sakoda, Y., Hatta, M. (2009). In vitro and in vivo characterization of new swine-origin H1N1 influenza viruses. *Nature 460*, 1021–1025.

Iwatsuki-Horimoto, K., Nakajima, N., Kiso, M., Takahashi, K., Ito, M., Inoue, T., Horiuchi M., Okahara N., Sasaki E., Hasegawa H an Kawaoka, Y. (2018). The marmoset as an animal model of influenza: infection with A (H1N1) pdm09 and highly pathogenic A (H5N1) viruses via the conventional or tracheal spray route. *Frontiers in microbiology, 9.* :844.

Jegede, A., Fu, Q., Lin, M., Kumar, A., & Guan, J. (2019). Aerosol exposure enhanced infection of low pathogenic avian influenza viruses in chickens. *Transboundary and Emerging Diseases*, 66(1), 435-444.

Josset, L., Engelmann, F., Haberthur, K., Kelly, S., Park, B., Kawoaka, Y. (2012). Increased viral loads and exacerbated innate host responses in aged macaques infected with the 2009 pandemic H1N1 influenza A virus. *Journal of virology, 86(20),* 11115-11127.

Kiso, M., Takahashi, K., Sakai-Tagawa, Y., Shinya, K., Sakabe, S., Le, Q. M. (2010). T-705

(favipiravir) activity against lethal H5N1 influenza A viruses. *Proceedings of the National Academy of Sciences, 107(2),* 882-887.

Kuiken, T., Rimmelzwaan, G. F., Van Amerongen, G., and Osterhaus, A. D. (2003). Pathology of human influenza A (H5N1) virus infection in cynomolgus macaques (Macaca fascicularis). *Veterinary pathology, 40(3),* 304-310.

Marriott, A. C., Dennis, M., Kane, J. A., Gooch, K. E., Hatch, G., Sharpe, S. (2016). Influenza A virus challenge models in cynomolgus macaques using the authentic inhaled aerosol and intra-nasal routes of infection. *PLoS One* 11:e0157887.

Safronetz, D., Rockx, B., Feldmann, F., Belisle, S. E., Palermo, R. E., Brining, D. (2011). Pandemic swine-origin H1N1 influenza A virus isolates show heterogeneous virulence in macaques. *Journal of virology, 85(3),* 1214-1223.

Shichinohe, S., Itoh, Y., Nakayama, M., Ozaki, H., Soda, K., Ishigaki, H.(2016). Comparison of pathogenicities of H7 avian influenza viruses via intranasal and conjunctival inoculation in cynomolgus macaques. *Virology* 493, 31–38.

Wonderlich, E. R., Swan, Z. D., Bissel, S. J., Hartman, A. L., Carney, J. P., O'Malley, K. J., ... & Frye, L. J. (2017). Widespread virus replication in alveoli drives acute respiratory distress syndrome in aerosolized H5N1 influenza infection of macaques. *The Journal of Immunology,* 198(4), 1616-1626.

Weinfurter, J. T., Brunner, K., Capuano, S. V. III, Li, C., Broman, K. W., Kawaoka, Y. (2011). Cross-reactive T cells are involved in rapid clearance of 2009 pandemic H1N1 influenza virus in nonhuman primates. *PLoS pathogens, 7*(11), e1002381.

Wonderlich, E. R., Swan, Z. D., Bissel, S. J., Hartman, A. L., Carney, J. P., O'Malley, K. J.(2017). Widespread virus replication in alveoli drives acute respiratory distress syndrome in aerosolized H5N1 influenza infection of macaques. *JThe Journal of Immunology, 198*(4), 1616-1626.

Wright, P. F., Neumann, G., and Kawaoka, Y. (2013). "Orthomyxoviruses," in Fields Virology, ed. *H. P. Knipe* (Philadelphia, PA: Lippincott Williams & Wilkins), 1186–1243.

七、圖表

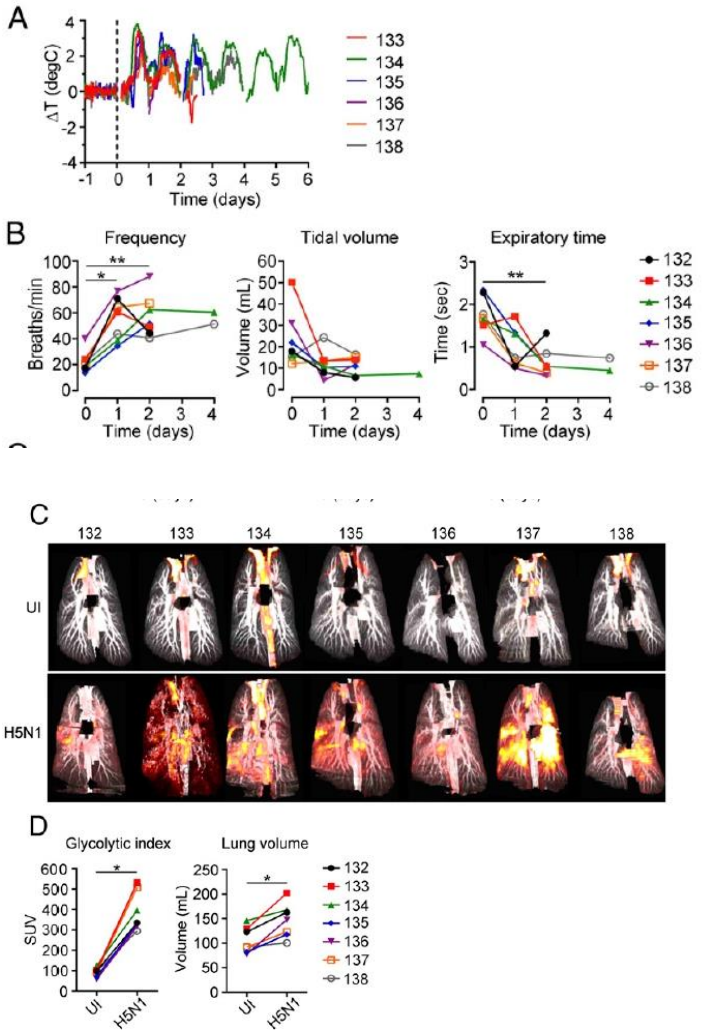

1 **FIGURE 1**. Aerosolized H5N1 infection of macaques produces fulminant bilateral
2 pneumonia. (A) Residual temperature differences relative to preinfection baseline values
3 determined by radiotelemetry. (B) Respiratory rate, tidal volume, and expiratory time
4 following H5N1 infection measured by plethysmography. (C) Paired combined PET-CT
5 images from each animal taken prior to infection (UI) and at 2 d after H5N1 infection. Red
6 coloration indicates FDG uptake. (D) Quantification of lung FDG uptake measured as
7 standardized uptake value (SUV) and of lung volume before and at 2 d after H5N1 infection.
8 The p values were determined through Friedman tests, followed by a Dunn multiple
9 comparison test (B) and Wilcoxon matched-pairs signed rank test (D). *p , 0.05, **p , 0.01.
10 SUV, standardized uptake value; UI, uninfected.

(Wonderlich *et al.*, 2017)

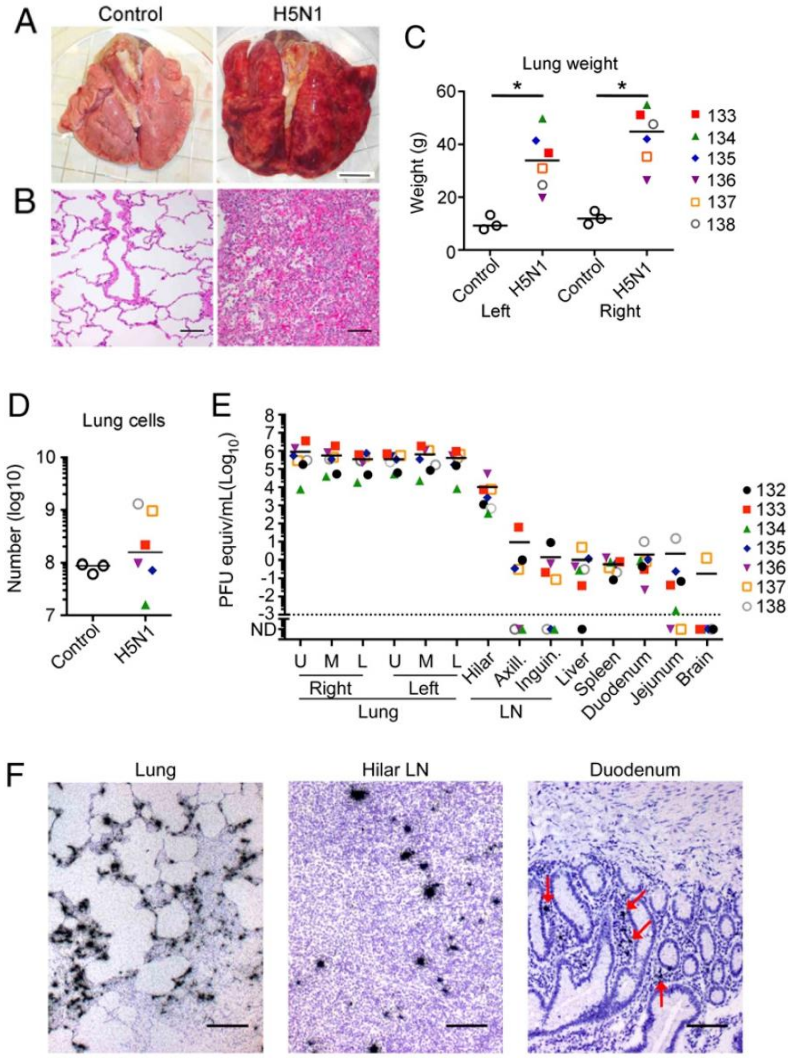

FIGURE 2. Profound lung inflammation and systemic infection following aerosolized H5N1 virus exposure. (A) Lungs from an uninfected control and H5N1-infected macaque. Scale bar, 2 cm. (B) H&E staining of control and H5N1-infected lungs at day 2 PI. Scale bars, 100 mm. (C) Lung weights at necropsy. (D) Total number of cells yielded from enzymatic digestion of lungs. (E) Semiquantitative real-time RT-PCR of influenza virus in homogenized tissues. (F) In situ hybridization of paraffinembedded sections from upper lung, hilar lymph node, and duodenum at day 2 PI. Influenza virus RNA is seen as dark grains in the walls of most alveoli, in the lymph node paracortex, and in duodenum lamina propria (red arrows). Counterstaining of lung sections reveals fluid accumulation in alveolar spaces. Scale bars, 100 mm. Horizontal lines in graphs represent medians. The p values were determined through Mann–Whitney U tests. *p , 0.05. L, lower; M, middle; ND, not detected; U, upper.

(Wonderlich *et al.*, 2017)

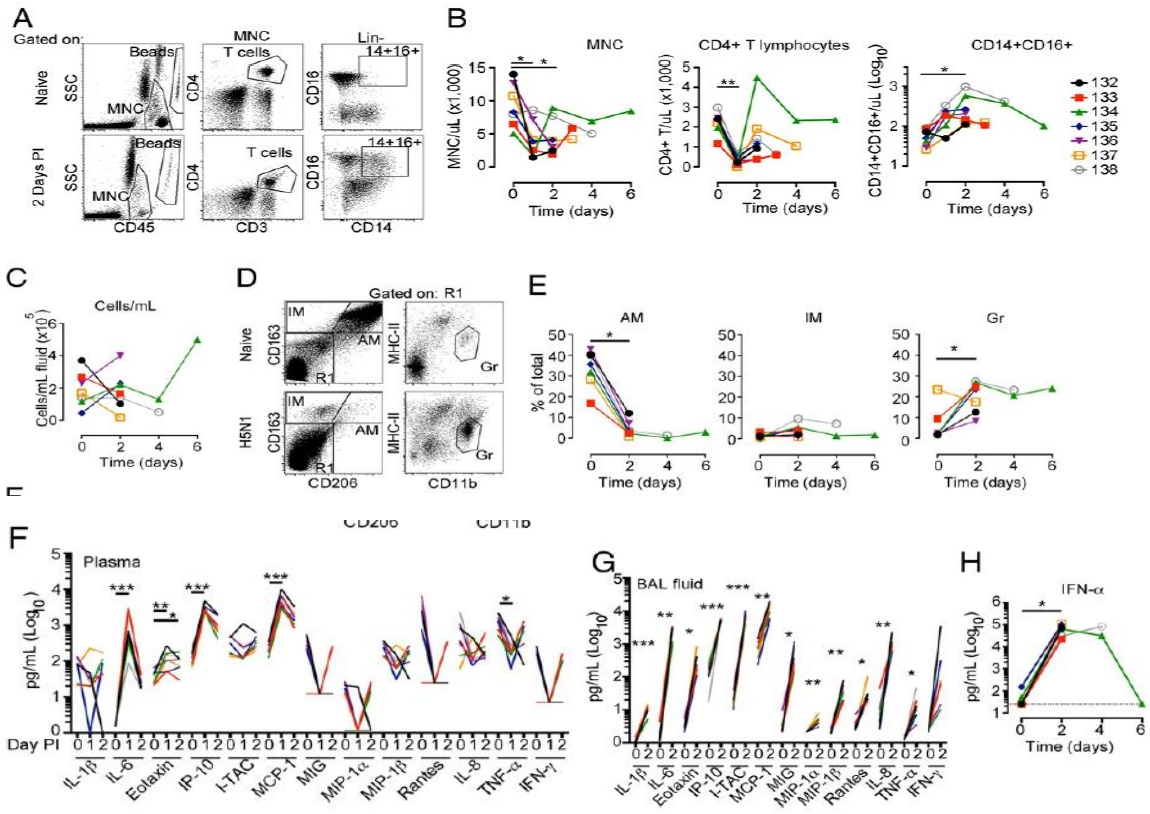

FIGURE 3. Innate immune response in blood and BAL following aerosolized H5N1 virus infection. (A) Gating strategy to identify blood mononuclear cells (MNC, CD45+), CD4+ T lymphocytes (T cells, CD45+ CD3+ CD4+), and intermediate monocytes (CD45+ CD32CD202HLA-DR+ CD14+ CD16+) by flow cytometry. (B) Quantification of MNC, CD4+ T lymphocytes, and intermediate monocytes (CD14+ CD16+) in blood. (C) Quantitation of cells in BAL fluid. (D) Gating strategy to identify alveolar macrophages (AM, CD163+ CD206+), interstitial macrophages (IM, CD163+ CD2062), and granulocytes (Gr, CD1632CD2062CD11b+ HLA-DR2) in BAL fluid by flow cytometry. (E) Quantification of AM, IM, and Gr in BAL samples. (F) Cytokine concentrations measured in the plasma and (G) BAL fluid through flow cytometric cytokine bead array. (H) IFN-a2 concentrations in BAL fluid as measured by ELISA. The p values were determined through Friedman tests, followed by Dunn multiple comparison tests (B and F), a Wilcoxon matched-pairs signed rank test (E and H), and a paired t test (G). *p , 0.05, **p , 0.01, ***p , 0.001. AM, alveolar macrophage; Gr, granulocyte; IM, interstitial macrophage; MNC, mononuclear cell.

(Wonderlich *et al.*, 2017)

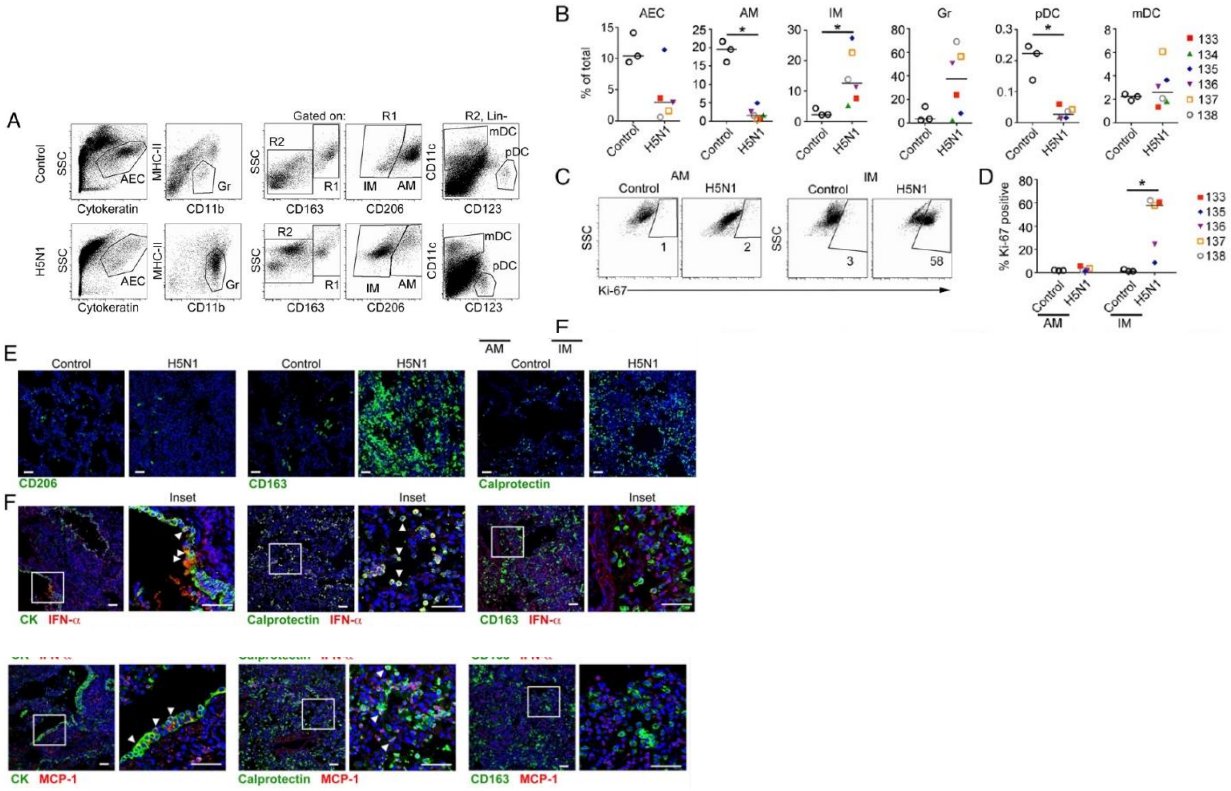

1 **FIGURE 4.** H5N1 infection leads to decimation of alveolar macrophages and infiltration of
2 interstitial macrophages and neutrophils. (A) Gating strategy to identify AEC (cytokeratin+),
3 neutrophils (granulocytes [Gr], CD11b+ HLA-DR2), alveolar macrophages (AM, CD163+
4 CD206+), interstitial macrophages (IM, CD163+ CD2062), plasmacytoid DC (pDC;
5 Lin2[CD3/CD20]HLA-DR+ CD1632CD123+), and myeloid DC (mDC;
6 Lin2[CD3/CD20]HLA-DR+ CD1632CD11c+) in lung suspensions by flow cytometry. (B)
7 Quantification of AEC, Gr, AM, IM, pDC, and mDC in lung suspensions. (C) Ki-67 staining
8 in alveolar macrophages and interstitial macrophages as measured through flow cytometry.
9 Numbers represent the percentage of each cell type expressing Ki-67. (D) Quantification of
10 Ki-67 expression on alveolar and interstitial macrophages. (E) Immunofluorescence staining
11 of lung sections from control and H5N1- infected macaques using the indicated Abs. Scale
12 bars, 50 mm. (F) Lung sections stained with Abs to cytokeratin (identifying AEC),
13 calprotectin (neutrophils), and CD163 (interstitial macrophages) and either IFN-a (top panels)
14 or MCP-1 (bottom panels). Arrowheads indicate cells costained for cellular markers and
15 cytokines. Scale bars, 50 mm. Horizontal lines in graphs represent medians. The p values
16 were determined through Mann–Whitney U tests. *p , 0.05. AM, alveolar macrophage; Gr,
17 granulocyte; IM, interstitial macrophage; mDC, myeloid DC; pDC, plasmacytoid DC.

(Wonderlich *et al.*, 2017)

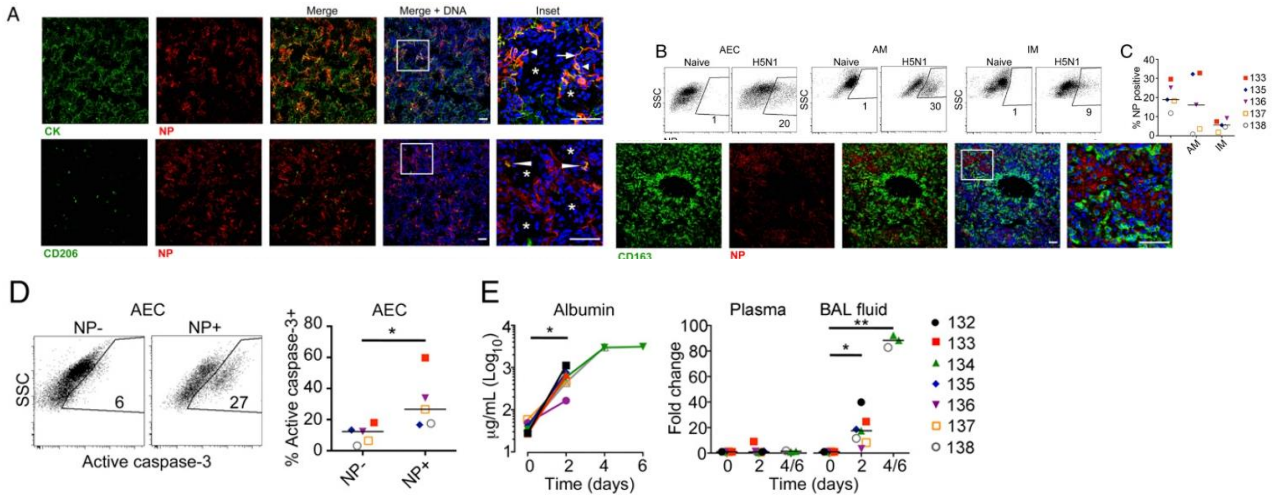

FIGURE 5. H5N1 infects AEC and alveolar macrophages and causes plasma leakage into airways. (A) Lung sections costained with Abs to cytokeratin (CK), CD206, or CD163 and H5N1 nucleoprotein (NP). Arrow indicates infected type I pneumocytes, and arrowhead indicates infected type II pneumocytes. Narrow arrowhead indicates infected alveolar macrophages. White stars mark alveolar spaces containing nucleated cells, identified by blue staining. Scale bars, 50 mm. (B) Flow cytometric analysis of nucleoprotein expression in AEC, alveolar macrophages (AM), and interstitial macrophages (IM) in naive or H5N1-infected lung. Numbers represent percentage of each cell type expressing nucleoprotein. Gating is based on staining of naïve samples stained for H5N1. (C) Quantification of nucleoprotein+ AEC, AM, and IM. (D) Flow cytometric analysis of active caspase-3 expression in AEC from an infected macaque costained for nucleoprotein expression. (E) Albumin concentration in BAL fluid and fold increase in albumin concentration relative to preinfection concentrations in plasma and BAL fluid. Horizontal lines in graphs represent medians. The p value was determined through a Wilcoxon matched-pairs signed rank test (D and E) and a Kruskal–Wallis test followed by a Dunn multiple comparison test (E). *p , 0.05, **p , 0.01. AM, alveolar macrophage; CK, cytokeratin; IM, interstitial macrophage; NP, nucleoprotein.

(Wonderlich *et al.*, 2017)

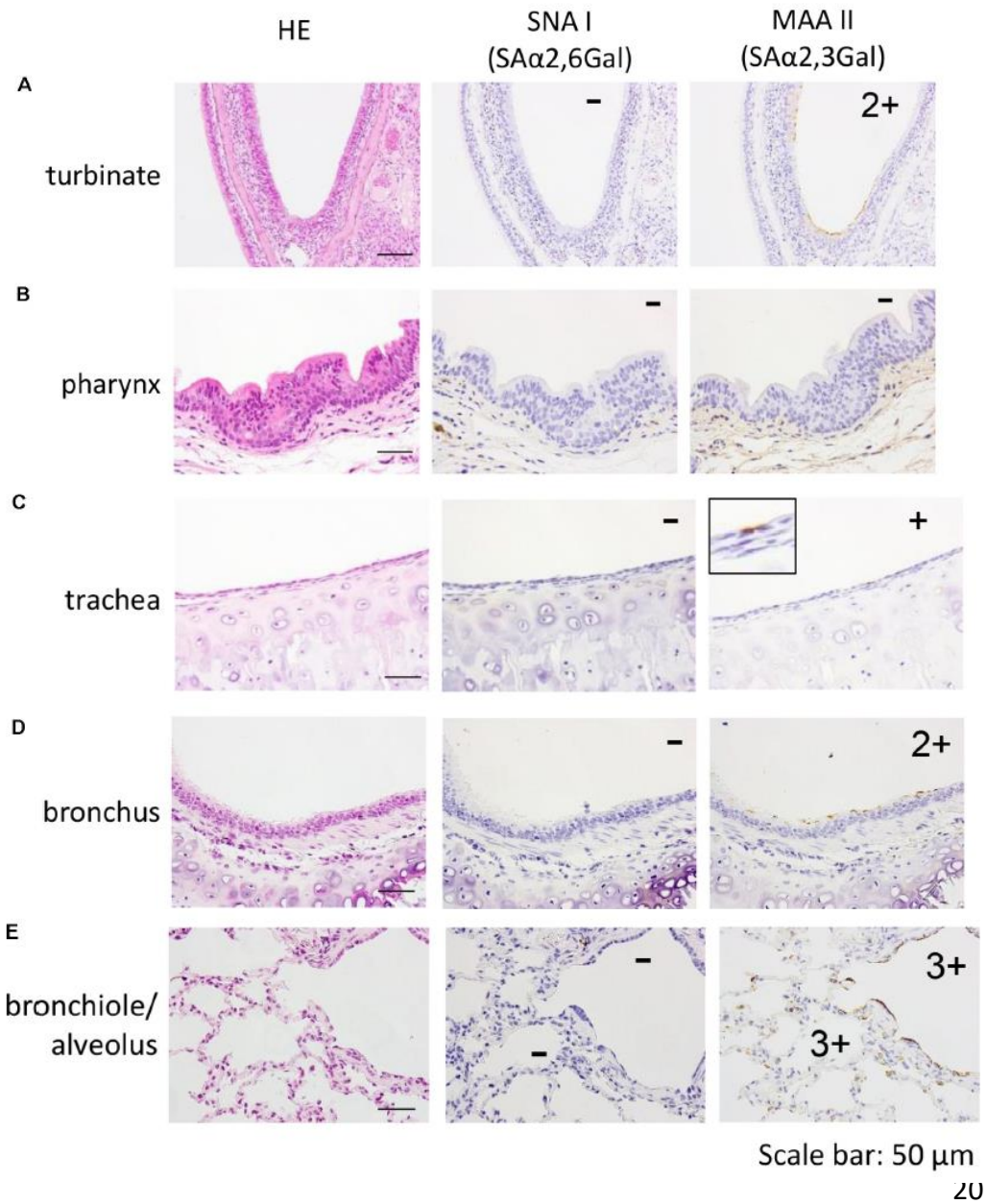

20

21 **FIGURE 6**. Detection of SAa2,6Gal and SAa2,3Gal oligosaccharides in the nasal turbinate
22 (A), pharynx (B), trachea (C), bronchus (D), and bronchiole/alveolar (E)of a 5-year-old
23 marmoset. No section reacted with SNA I (A–E, center). In contrast, MAA II reacted with
24 epithelial cells in the nasal turbinate, trachea, bronchus,bronchiole, and alveolus (A,C–E,
25 right). Quantification of MAA II-positive cells in each section: none (–), a few (+), several
26 and partial (2+), many and diffuse (3+).

27

28

(Iwatsuki-Horimoto et al., 2018)

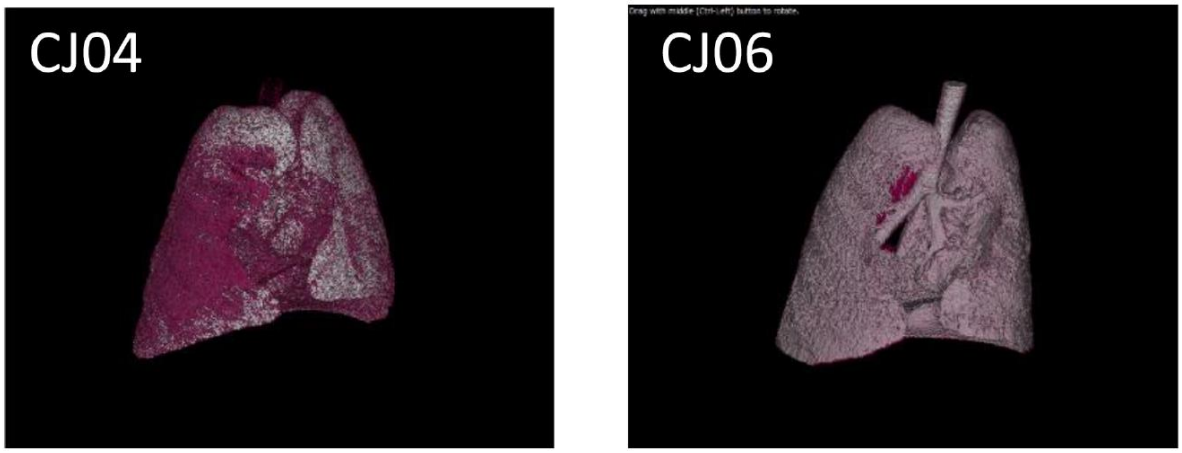

FIGURE 7. Micro-CT of VN1203-infected marmosets. CJ04 was infected via the tracheal spray route; CJ06 was infected via the conventional route. Images of the lungs of marmosets CJ04 and CJ06 on 3 dpi. The pink color indicates inflamed areas.

(Iwatsuki-Horimoto et al., 2018)

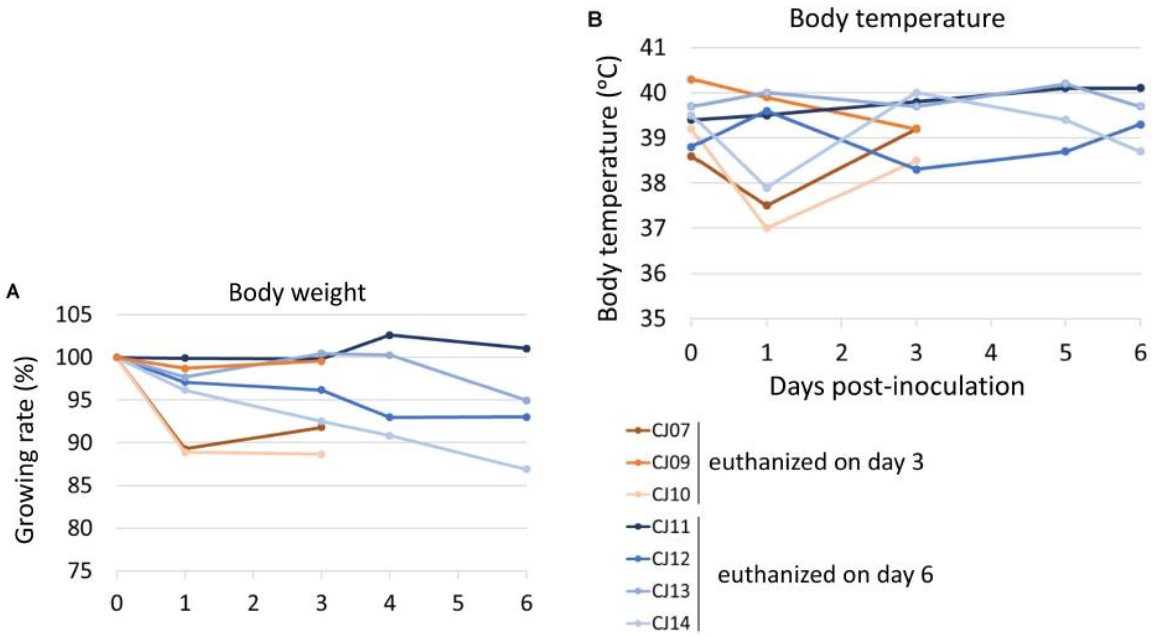

FIGURE 8. Change in body weight (A) and body temperature (B) of VN1203-infected marmosets. On 0 (the day of infection), 1, 3, 5, and 6 dpi, the body weight (A) and temperature (B) of each marmoset was measured. Three (CJ07, CJ09, and CJ10) or four (CJ11, CJ12, CJ13, and CJ14) marmosets were euthanized on 3 or 6 dpi, respectively.

(Iwatsuki-Horimoto et al., 2018)

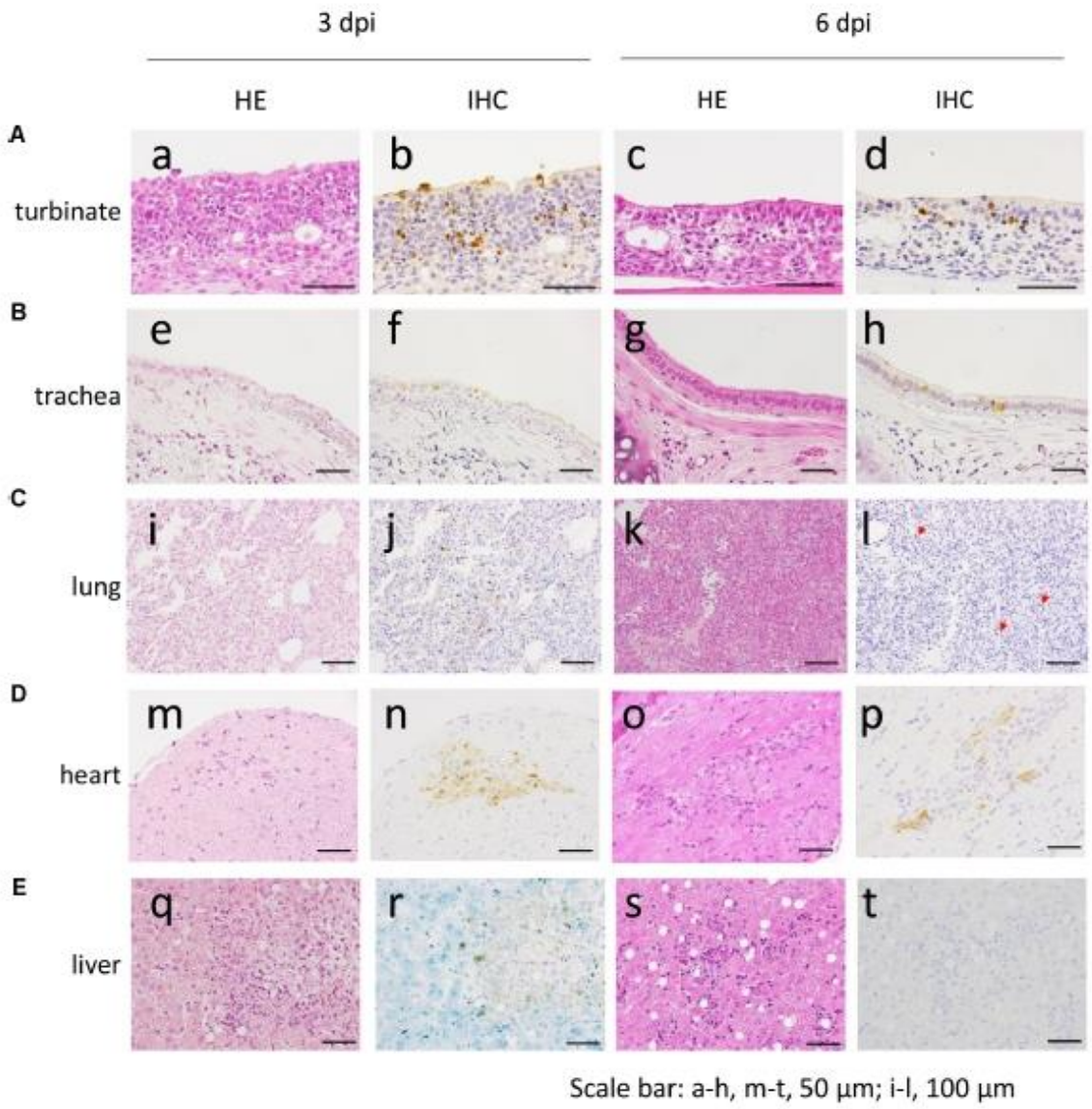

FIGURE 9. Pathological examination of the nasal turbinate **(A)**, trachea **(B)**, lung **(C)**, heart **(D)**, and liver **(E)** of VN1203-infected marmosets. a, b, m, n, CJ09; c, d, s, t, CJ11; e, f, i, j, q, r, CJ07; g, h, CJ14; k, l, CJ13; o, p, CJ12. Red arrows in (l) indicate antigen-positive cells. HE, hematoxylin and eosin staining; IHC, immunohistochemistry for the detection of influenza virus NP antigen.

(Iwatsuki-Horimoto et al., 2018)

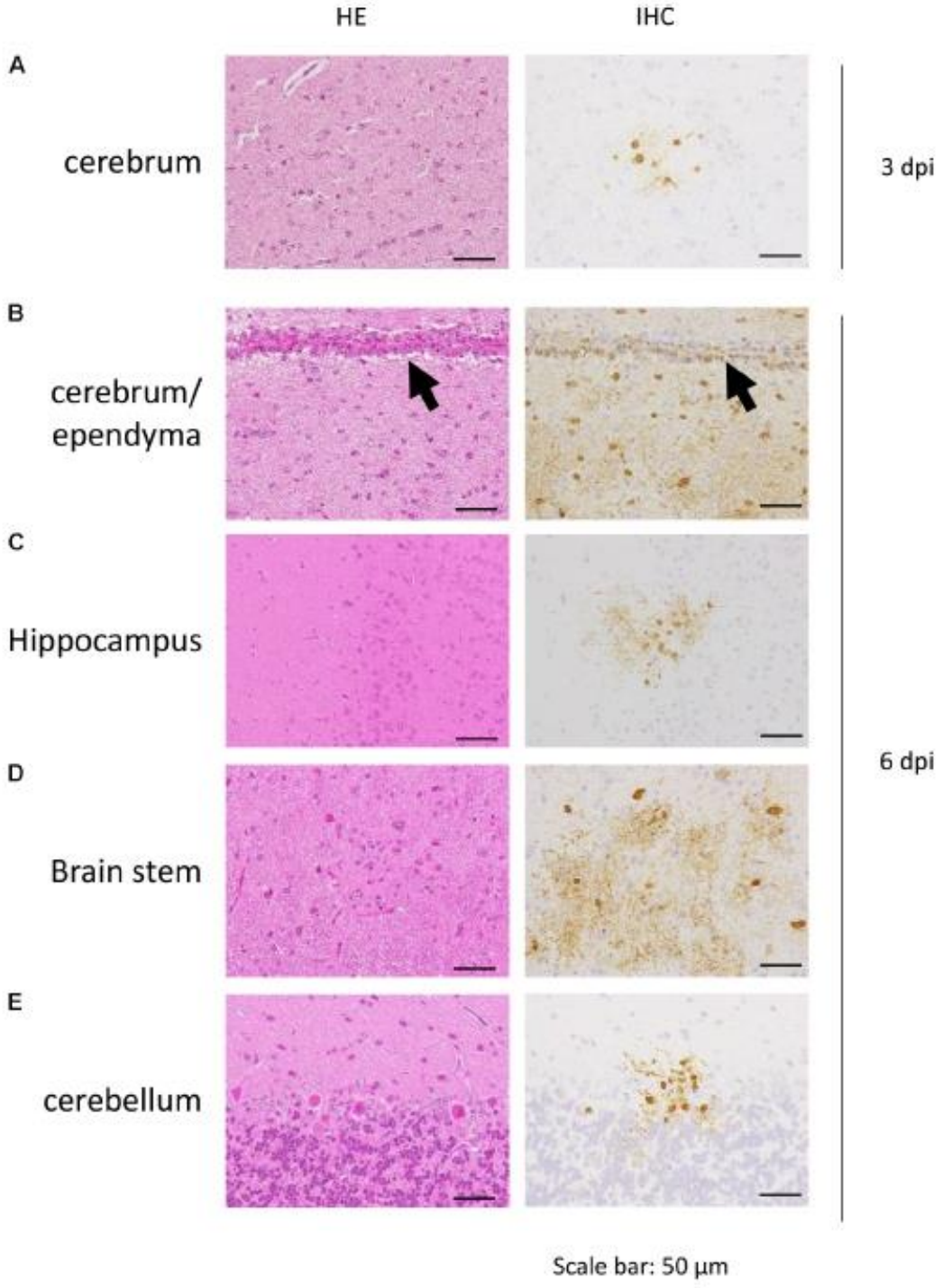

FIGURE 10. Pathological examination of marmoset brain. Cerebrum of CJ07 (A), cerebrum of CJ14 (B), hippocampus of CJ14 (C), brain stem of CJ13 (D), and cerebellum of CJ13 (E), which were infected with VN1203. Black arrows in (B) indicate ependyma. HE, hematoxylin and eosin staining; IHC, immunohistochemistry for the detection of influenza virus NP antigen.

(Iwatsuki-Horimoto et al., 2018)

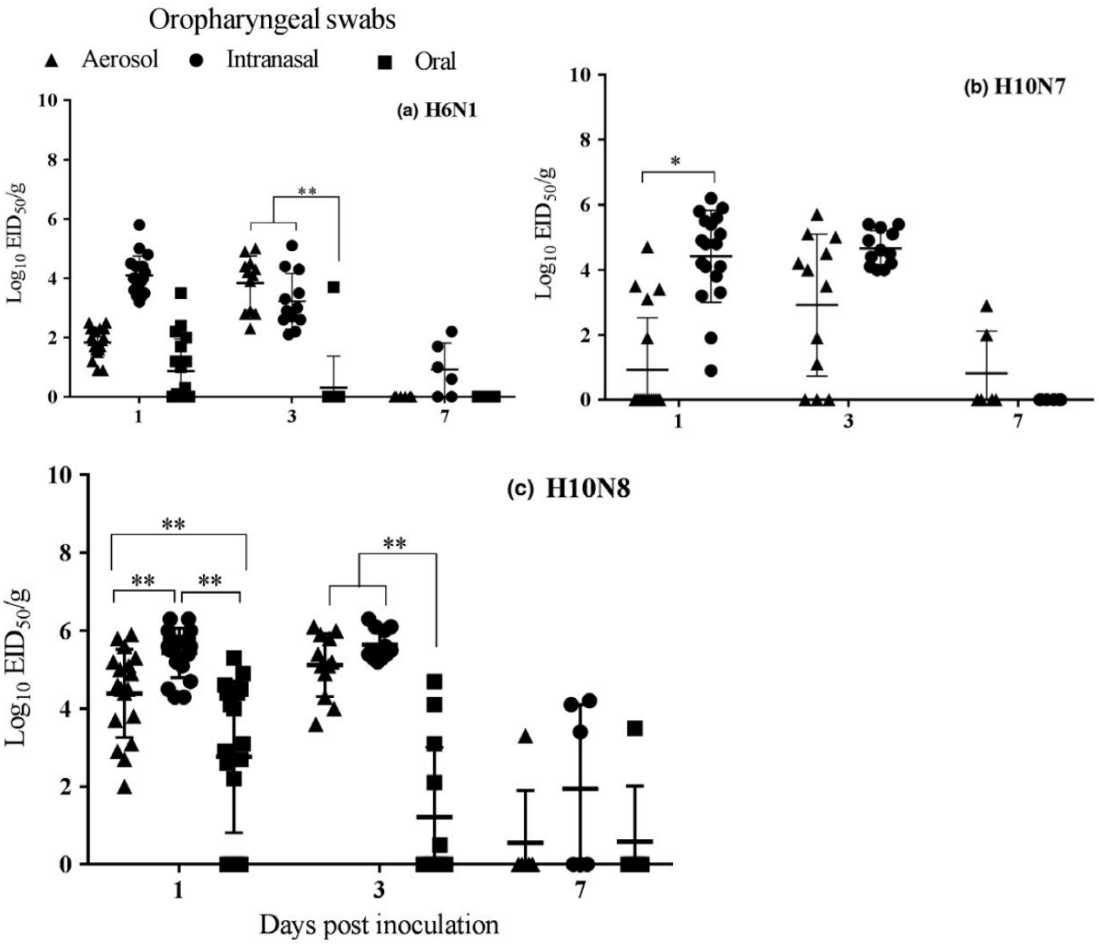

Figure 11. Virus replication in oropharyngeal cavity of chickens inoculated with H6N1 (a), H10N7 (b), and H10N8 (c) virus via the aerosol (▲), intranasal (●), or oral (■) route. Data represent the mean viral titres (± *SD*) in swabs (*n* = 18, 12, 6 on 1, 3, 7 days postinoculation respectively). *($p < 0.05$) and **($p < 0.01$) represent significant differences between groups

(Jegede *et al*., 2018)

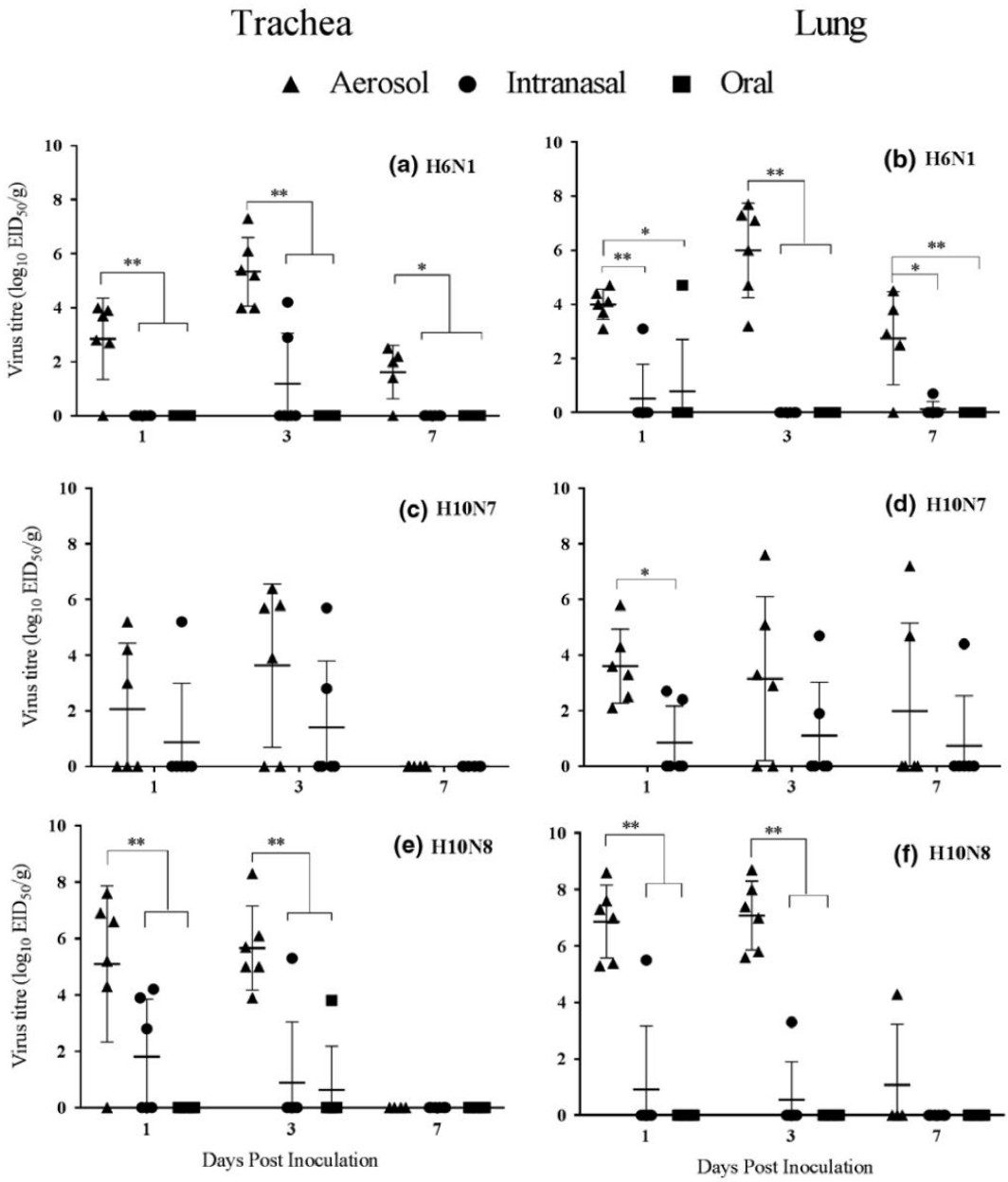

FIGURE 12. Virus replication in tracheal and lung tissues of chickens inoculated with H6N1 (a, b), H10N7 (c, d), and H10N8 (e, f) virus via the aerosol (▲), intranasal (●), or oral (■) route. Data represent the mean viral titres (± SD) in tissue specimens (n = 6). *($p < 0.05$) and **($p < 0.01$) represent significant differences between groups

(Jegede *et al*., 2018)

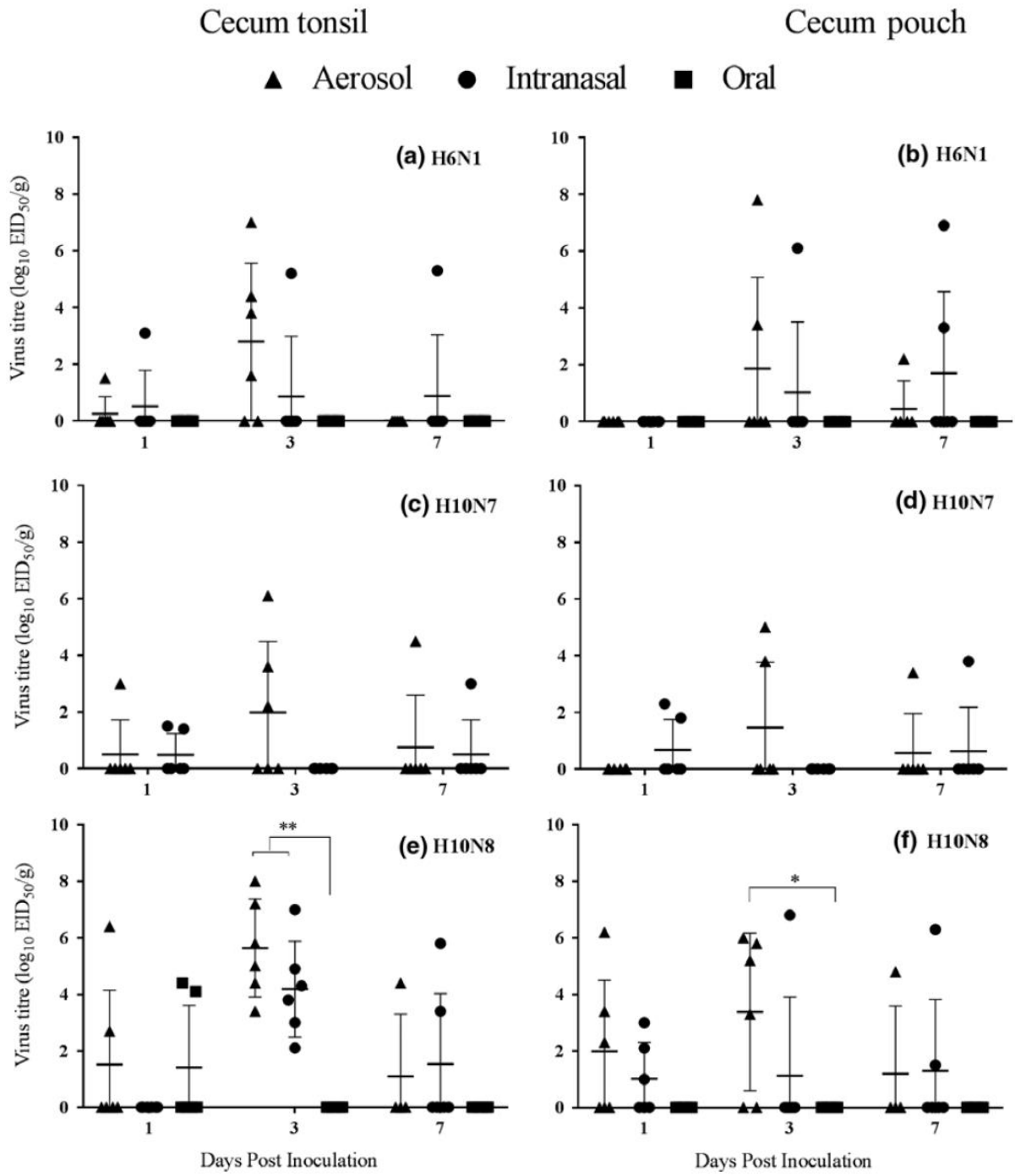

FIGURE 13. Virus replication in ceca of chickens inoculated with H6N1 (a, b), H10N7 (c, d), and H10N8 (e, f) virus via the aerosol (▲), intranasal (●), or oral (■) route. Data represent the mean viral titres (± SD) in tissue specimens (n = 6). *($p < 0.05$) and **($p < 0.01$) represent significant differences between groups

(Jegede *et al*., 2018)

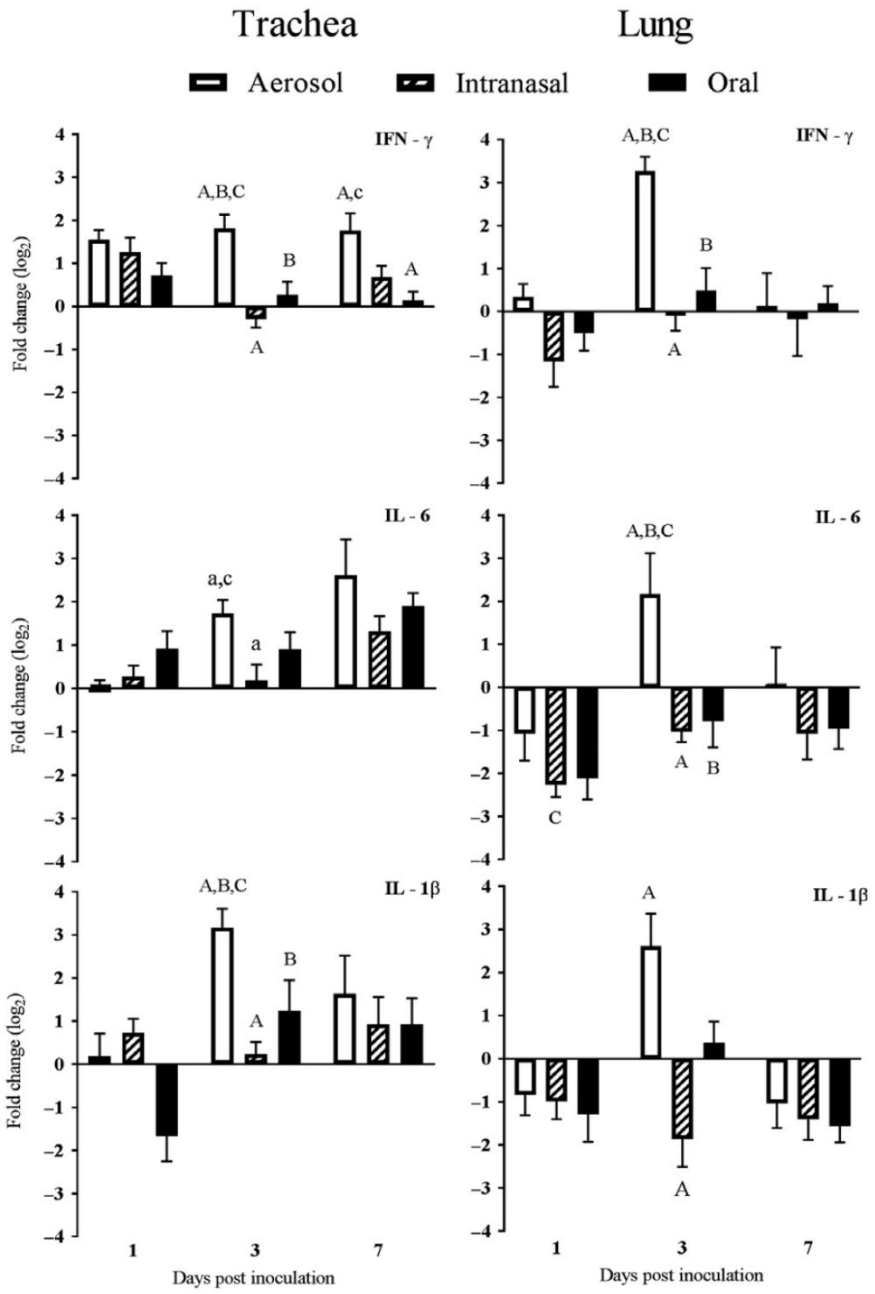

FIGURE 14. Cytokine mRNA response in chicken trachea and lung to H6N1 inoculation via the aerosol (white bar), intranasal (striped bar), or oral (dark bar) route. Cytokine mRNA expressions (n = 6) were measured by quantitative PCR with reference to the expression of GAPDH gene, and were presented as the mean fold change (± SEM) compared with values in control chickens (inoculated with PBS). Statistical analysis was performed by comparing cytokine mRNA expressions in control and inoculated chickens. Bars with the same letter of A or B ($p < 0.01$), a or b ($p < 0.05$) are significantly different, and letters C ($p < 0.01$) and c ($p < 0.05$) represent significant difference from the control (Jegede *et al*., 2018)

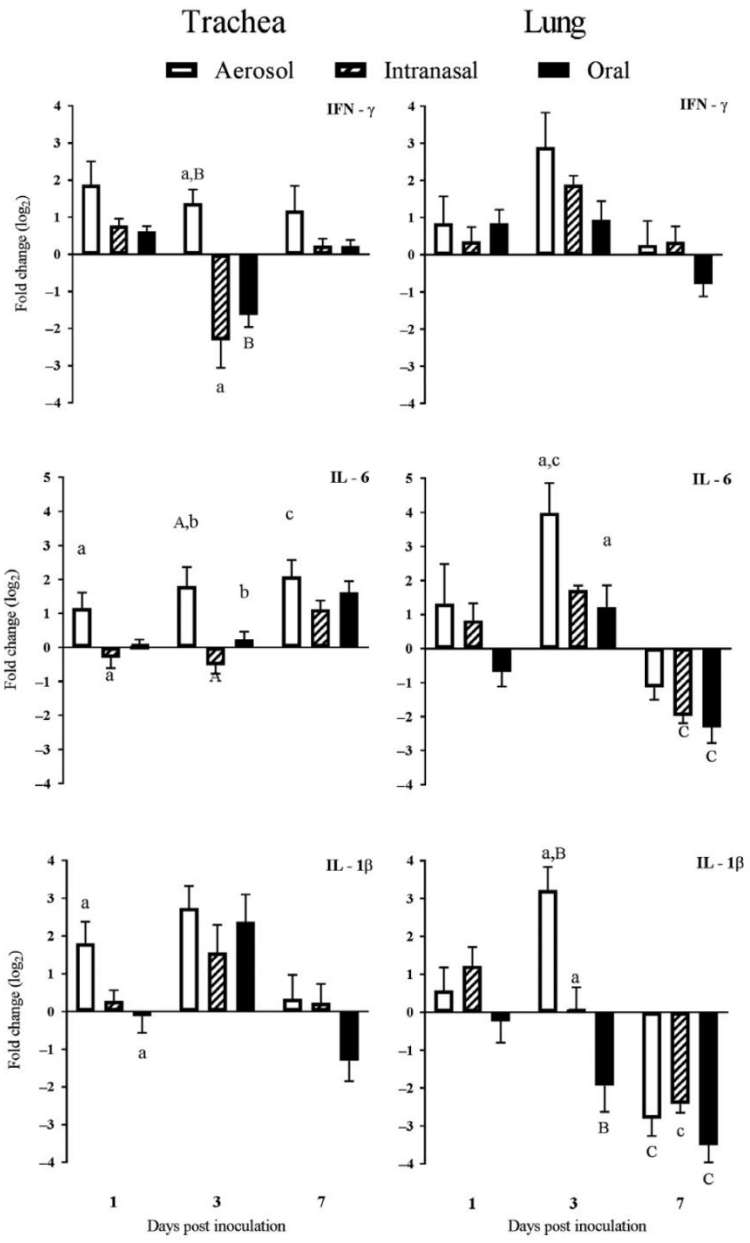

FIGURE 15. Cytokine mRNA response in chicken trachea and lung to H10N8 inoculation via the aerosol (white bar), intranasal (striped bar) or oral (dark bar) route. Cytokine mRNA expressions (n = 6) were measured by quantitative PCR with reference to the expression of GAPDH gene, and were presented as the mean fold change (± SEM) compared with values in control chickens (inoculated with PBS). Statistical analysis was performed by comparing cytokine mRNA expressions in control and inoculated chickens. Bars with the same letter of A or B ($p < 0.01$), a or b ($p < 0.05$) are significantly different, and letters C ($p < 0.01$) and c ($p < 0.05$) represent significant difference from the control

(Jegede *et al*., 2018)

Table 1. Characteristics of infection and virus titers

(Wonderlich *et al.*, 2017)

Animal ID	Virus Dose (log_{10} PFU)	Time to Death (d)	Virus Titer (log_{10} PFU/ml or PFU/g)												
			Nasal Wash				BAL			Left Lung			Right Lung		
			Day 1	Day 2	Day 4	Day 6	Day 2	Day 4	Day 6	Upper	Middle	Lower	Upper	Middle	Lower
132	7.26	3	0.70	0	—	—	3.04	—	—	3.73	4.33	4.25	4.23	4.36	4.79
133	7.17	2[a]	1.81	1.00	—	—	4.03	—	—	7.26	6.64	6.79	6.73	4.60	7.80
134	7.07	6[a]	1.40	3.18	1.00	0	7.45	5.13	4.96	6.69	5.77	3.00	5.72	6.03	3.65
135	6.16	3	2.05	3.81	—	—	3.10	—	—	5.39	5.56	5.75	5.56	5.77	5.85
136	6.46	2[a]	0	0	—	—	3.47	—	—	5.86	5.66	5.29	5.36	5.91	4.98
137	6.37	2[a]	0	0	—	—	3.63	—	—	5.29	5.73	5.64	5.66	5.76	5.61
138	6.57	4	0	0.48	0	—	3.33	3.67	—	4.57	5.23	5.51	4.85	5.37	4.20
Mean	6.72	3.2	0.85	1.21	0.50	0	4.01	4.40	4.96	5.54	5.56	5.18	5.44	5.40	5.27

[a]Humanely sacrificed.

—, not available

TABLE 2. Virus titers in the nasal aspirate of marmosets infected with Osaka164[a].

(Iwatsuki-Horimoto et al., 2018)

Inoculation route	Animal ID	Virus titers (log_{10}PFU/ml)						
		Days post-inoculation						
		1	3	5	7	9	11	13
Tracheal spray route	CJ03	–	–	–	–	–	–	–
	CJ04	1.4	4.7	–	3.2	–	–	–
Conventional route	CJ05	1.0	1.8	2.1	–	5.2	1.3	–
	CJ06	1.6	3.7	2.8	2.4	–	–	–

[a]*Four- to eight-year-old female marmosets were anesthetized and inoculated with 1.0 × 10^7 PFU (in 200 μl) of Osaka164 via the tracheal spray route (CJ03 and CJ04) or via the conventional route (CJ05 and CJ06). Under anesthesia, nasal aspirates from each marmoset were collected every other day for virus titration.*

1 **TABLE 3.** Virus titers in organs of infected marmosetsa.

2 (Iwatsuki-Horimoto et al., 2018)

Organs		Virus titers (log_{10}PFU/g)						
		3 dpi			6 dpi			
		CJ07	CJ09	CJ10	CJ11	CJ12	CJ13	CJ14
Left lung	Cranial	7.2	3.3	6.7	–[b]	–	3.2	–
	Caudal	6.2	3.9	6.6	–	–	2.9	–
Right lung	Cranial	6.7	4.1	6.8	–	3.7	3.9	–
	Middle	7.6	5.5	5.6	–	2.7	2.7	–
	Caudal	8.0	4.0	6.2	–	4.3	2.7	–
	Accessary	7.3	3.7	6.5	–	–	–	–
Trachea		5.6	3.4	4.7	–	6.0	2.4	3.0
Left bronchus		7.7	3.2	6.9	–	3.3	5.0	3.4
Nasal turbinate		6.1	5.7	4.6	5.3	–	6.5	4.4
Cerebrum	Frontal	–	–	–	–	–	–	3.0
	Temporal	–	–	–	–	–	–	3.2
	Parietal	–	–	–	–	–	–	3.3
	Occipital	–	–	–	–	–	–	4.4
Brain stem		–	–	–	–	–	–	6.8
Olfactory bulb		–	–	–	–	–	–	4.9
Cerebellum		4.5	–	–	–	–	3.7	5.1
Heart		4.2	3.4	3.6	–	–	–	–
Liver		4.7	–	3.2	–	–	–	–
Duodenum		4.6	4.5	4.0	–	–	–	–
Colon		4.2	–	6.0	–	–	–	2.0
Spleen		3.8	–	4.1	–	–	2.7	–
Kidney		4.2	–	2.2	–	–	–	–
Serum		–	–	–	–	–	–	–
Whole blood		ND[c]	ND	ND	–	–	–	–

[a]Marmosets were inoculated with 1.0 × 10^7 PFU (in 200 μl) of VN1203 A(H5N1) via the tracheal spray route; [b]–, virus not detected (detection limit: 1.0 log_{10}PFU/ml); [c]ND, not done.

TABLE 4A. Pathologic scores[a;b] of respiratory organs by hematoxylin and eosin staining (HE) and the number of antigen-positive cells[c] by immunohistochemistry (IHC) in VN1203-infected marmosets.

(Iwatsuki-Horimoto et al., 2018)

Organs		3 dpi						6 dpi							
		CJ07		CJ09		CJ10		CJ11		CJ12		CJ13		CJ14	
		HE	IHC	HE	IHC	HE	IHC	HE	IHC	HE	IHC	HE	IHC	HE	IHC
Left lung	Cranial	4	+	3	–	5	+	4	–[b]	4	–	5	–	3	–
	Caudal	4	+	3	–	5	+	3	–	4	–	5	–	4	–
Right lung	Cranial	4	+	3	–	5	+	3	–	5	+	4	+	5	–
	Middle	4	+	3	–	4	+	3	–	5	–	5	+	4	–
	Caudal	3	+	3	–	5	+	3	–	5	–	5	–	5	–
	Accessary	NA[d]	NA	NA	NA	NA	NA	NA	NA	NA	NA	NA	NA	NA	NA
Trachea		1	+	1	–	1	–	1	–	1	+	1	–	1	+
Nasal turbinate		1	+	1	+	2	+	1	+	1	–	1	+	1	+

[a]Lung: –, no apparent changes; 1, minimal changes; 2, slight inflammation; 3, mild inflammation including infiltration of neutrophils, monocytes/macrophages, or lymphocytes; 4, moderate inflammation (>50% of sections examined); 5, marked inflammation including edema and fibrin transudation. The area with edema and fibrin transudation represents <50% of the section examined; 6, severe inflammation. The area with edema and fibrin transudation represents >50% of the section examined. [b]Trachea and nasal turbinate: –, no apparent changes; 1, mild inflammation; 2, moderate inflammation; 3, severe inflammation. [c]Detection of influenza virus antigen in tissue sample sections. The extent of the abundance of virus-antigen-positive cells in the entire section of the sample was defined as follows: –, no antigen-positive cells found; +, 1–10 virus-antigen-positive cells found; ++, 11–101 virus-antigen-positive cells found; +++, > 101 virus-antigen-positive cells found. [d]NA, not available.

TABLE 4B. Pathologic scores[a] of non-respiratory organs by hematoxylin and eosin staining (HE) and the number of antigen-positive cells[b] by immunohistochemistry (IHC) in VN1203-infected marmosets.

(Iwatsuki-Horimoto et al., 2018)

Organs		3 dpi						6 dpi							
		CJ07		CJ09		CJ10		CJ11		CJ12		CJ13		CJ14	
		HE	IHC	HE	IHC	HE	IHC	HE	IHC	HE	IHC	HE	IHC	HE	IHC
Cerebrum	Frontal	–	–	–	–	–	–	–	–	–	–	–	–	–	+++
	Temporal	–	–	–	–	–	–	–	–	–	+	–	+	–	+++
	Parietal	–	+	–	–	1	–	–	–	–	–	–	–	–	+++
	Occipital	–	+	–	–	–	–	–	–	–	–	–	–	–	++
Brain stem		–	–	–	–	–	–	–	–	1	+	1	+	–	+++
Olfactory bulb		–	–	–	–	NA[c]	NA	–	–	–	–	–	–	–	–
Cerebellum		–	+	–	–	–	–	–	–	–	–	–	+	–	–
Heart		–	++	1	++	–	+	–	–	1	+	–	+	–	NA
Liver		1	++	–	–	1	+	1	–	–	–	–	–	–	–
Duodenum		–	–	–	–	–	–	–	–	–	–	NA	NA	NA	NA
Colon		–	–	–	–	–	–	–	–	–	–	–	–	–	–
Spleen		–	–	–	–	–	–	–	–	–	–	–	–	–	NA
Kidney		–	–	–	–	–	–	–	–	–	–	–	–	–	–

[a]–, No apparent changes; 1, mild inflammation; 2, moderate inflammation; 3, severe inflammation. [b]Detection of influenza virus antigen in tissue sample sections. The extent of the abundance of virus-antigen-positive cells in the entire section of the sample was defined as follows: –, no antigen-positive cells found; +, 1–10 virus-antigen-positive cells found; ++, 11–101 virus-antigen-positive cells found; +++, > 101 virus-antigen-positive cells found. [c]NA, not available.